

## Current-voltage measurements of Al/a-Se/Au Schottky diode solar cells

Mayyada M. Fdhala<sup>1</sup>, Ayser A. Hemed<sup>2,\*</sup>, Ramiz A. Al-Ansari<sup>3</sup>, Raad M. Al-Haddad<sup>4</sup>,  
Rasha S. Abbas<sup>5</sup>

<sup>1</sup> Distinguished girl secondary school, second Karkh directorate of education, Baghdad, IQ

<sup>2</sup> Dept. of Physics, college of education, Mustansiriyah University, Baghdad, I.Q.

<sup>3</sup> Dept. of Physics, College of Science for women, University of Baghdad, Baghdad, I.Q.

<sup>4</sup> Dept. of Physics, College of Science, Baghdad University, Baghdad, I.Q.

<sup>5</sup> First Karkh directorate of education, Baghdad, I.Q.

\*Corresponding author: ayser.hemed@uomustansiriyah.edu.iq

### Abstract

Schottky, S., diode Al/a-Se/Au as solar cells were made up by thermal evaporation technique on glass thin slide at a substrate under vacuum (vacuum value equal to  $10^{-5}$  mbar). The S. barriers have been prepared with different thicknesses (300,500 and 700) nm at room temperature and (343) K annealing temperature. The current-voltage (I-V) physical properties of the S. barrier have got that the rectification properties and approved as a solar cell which has been developing with the increasing (annealing temperature, A.T.s, and thickness of layers of S. diode). Experience under lighting shows good efficiency ( $\eta$ ), which increased linearly with both consistencies and AT from (0.0318% to 4.064%) and from (0.0318% to 0.4778%). This is for three values of lighting power density (160, 230, 400)  $mW/cm^2$  in which they behave is similarly. The best efficiency obtained in this work was (12.407)% at a power density of 230  $mW/cm^2$ , with thickness 500nm and 343K annealing T. Also (15.286)% at 400  $mW/cm^2$ , with thickness 700nm and 343K annealing T.

Keywords: Al/a-Se/Au; I-V measurements; Schottky diode; semiconductor-metal junction; solar cell.

### 1. Introduction

Semiconductor – semiconductor devices meet wide applications in laser diode and photodiode manufacturing. In this case, heterojunction is constructed for optical communications amplifiers, transmitter and receiver units, optical fiber sensors sources, scanners, printers, etc. related applications (Hemed et al., 2022; Hemed et al., 2021; Hemed & Abbas; 2020). Metal semiconductor constructions permanently include the deposition of metal films for two types of contacts: Ohmic and S. contact. These two contacts depend on the type of metal which is used. The metal-semiconductor M.S. junction, the surface preparations, the methods used to deposition, and thermal treatment for the thin film (Zeghbroeck 2004).

An MS junction is regarded as its current-voltage relationship; it is called an S. contact if it displays rectifying properties. While if it displays close to linear, in both directions and the resistance displays low, it is called an Ohmic contact, O.C.

Metal in the device is carried interested in contact with a semiconductor, a (potential barrier) is shaped at the M.S. interface. In 1938, S. advised that rectifying performance might arise from a potential barrier, so the semiconductor's constant space charges. That will be known by the S. Barrier model (SBM) (Sze 1981). However, M.S. devices can behave as non-rectifying performance. So, the contact can be negligible resistance regardless of the split of the practical Voltage. This contact is called an Ohmic contact (Parlakturk 2007). So that can be characterized experimentally for the S.M. junction by its current-voltage relationship (Sze 1981).

Solar cell device has a significant region P.N. junction used to transform the sunlit to electric current. This device uses the photovoltaic, P.V., effect by increasing photo-generated so that the minority carriers are separated via a junction by a built-in field. At the same time, most transports arrived on the opposite sides of the intersection. Then the concentration of majority carriers is responsible for creating Voltage through the external circuit. Work is done when circuit load closes, and a current circuit flows (Nelson 2003).

Getting a P.V. cell can have created several junctions as S. junction, made between semiconductors and metals. A heterojunction is formed between a semiconductor and another semiconductor under certain conditions. A solar cell, S.C., type of S. junction has an old history; since 1883, first one Charles Fritts used selenium (semiconductor) by coated with a gold (metal) thin layer of it to make the first S.C. in the world. Yet, scientists and researchers have commanded less care; metals in the active region design no general solar cell. However, in the past, university research to produce a new line has demonstrated that by depending on S. junction in designed solar cell and continue to be used honestly generally in a lab (McEvoy et al., 2003).

Common characteristics of PV SC (energy converter) are Current-Voltage (I-V) characteristics which can obtain by several means are: (a) P.N. junction. (b) the P.V. output. (c) the rectifier forward. The proper methods must be chosen for the individual application to get the correct information. Most commonly used is the P.V. output characteristic to determine solar converter performance. P.V. output characteristic is a fast method is described for getting on a characteristic for any light level so obtained at a different light level. P.V. output characteristic includes two coordinate translations. Requires only the knowledge of the series resistance and system, the difference in short circuit current or light intensities (Wolf & Rauschenach 1963).

On the other hand, the more favorable space vehicle-related applications are the GaAs-based SC than silicon-based. This is due to their being more efficient and better material resistant to thermal and mechanical degradation in their environments (Sumaryada *et al.*, 2019).

This study aims to prepare the S. diode, then the S. barrier (with gold as a metal). To study the amorphous selenium film's behavior inside the junctions. We are looking at amorphous - Se S. diode parameters: saturation current, ideality factor, and barrier height. From successful indications of the previous measurements, these devices operated during halogen illuminating, and different parameters (open circuit voltage and short circuit current also efficiency measurements) have been studied.

## 2. Experimental part

S. junction prepared by using corning glass as a substrate, the first step Al as an O.C. (300nm) has been evaporated, then Selenium (Se) layer with different thicknesses (300,500 and 700) nm. Thin films of Se were ready by the vacuum evaporation method for a-Se with purity equal to 99% and used high vacuum reach to  $5 \times 10^{-6}$  unit (mbar) on a glass substrate at room T. The deposition process happens with a constant deposition rate ( $= 0 \text{ \AA}/\text{sec}$ ). Se's optical, electrical, and structural properties have been studied experimentally by this reference (Mutar & Hemed 2014).

Last step, Au as an S. contact with the thickness (50nm), then this device is annealed to (343K) at 30 minutes. Before evaporating the S. junction, the Aluminum contact must identify behaviors as an O.C. Therefore, the I-V characteristics of Al/a-Se/Al in the darkness must be investigated a linear behavior between the Aluminum and Se. Further, Se's electron affinity ( $\chi_s$ ) is larger than the work function ( $\phi_B$ ) of the Aluminum and, consequently, the low barrier height induces between them. Then the S. metal contact (Au) has been evaporated with 50nm and then circle Gold layer chosen by evaporation to be as points (Fdhala 2011).

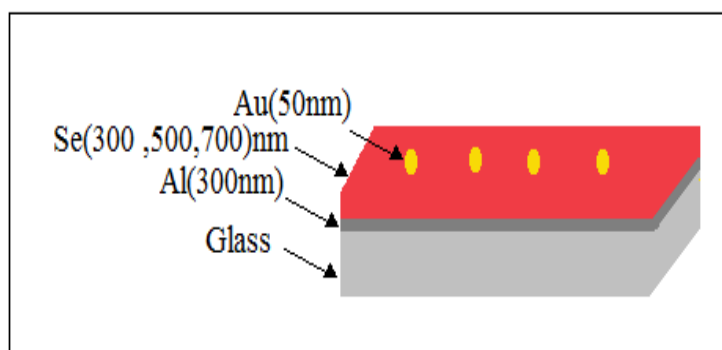


**Fig. 1.** The basic structure of typical Al/a-Se/Au S. diodes.

In figure (2),  $I - V$  characteristics of Au/a-Se/Al Junctions in forward and reverse bias was made by d.c. Power supply, digital Picometer, and voltmeter as shown. The bias voltage was changed from (0 – 1)V in forwarding and reverse discrimination. From  $I - V$  measurements, the potential barrier height ( $\phi_B$ ) can be determined by two important factors: ideality factor of the diode ( $n$ ) and the reverse saturation current ( $J_o$ ), by using this equation (Khan *et al.*, 1995).

$$I = I_o \left[ \exp \left( \frac{qV}{nkT} \right) - 1 \right] \quad \dots (1)$$

$$\text{where: } I = AA^* \exp \left( -\frac{q\phi_B}{k_B T} \right) \quad \dots (2)$$

From the above relationship for forwarding value of  $V$  in excess of  $3k_B T/q$ , when a plot of  $\ln(I)$  with  $V$  gets on a straight line. Then  $I_o$  gets on from the straight line when  $t_o = 0$ , and by knowing  $I_o$ ,  $A A^*$ , also the  $T$ , can be determined the barrier height (AbuShama *et al.*, 2002; Hamza, 2010).

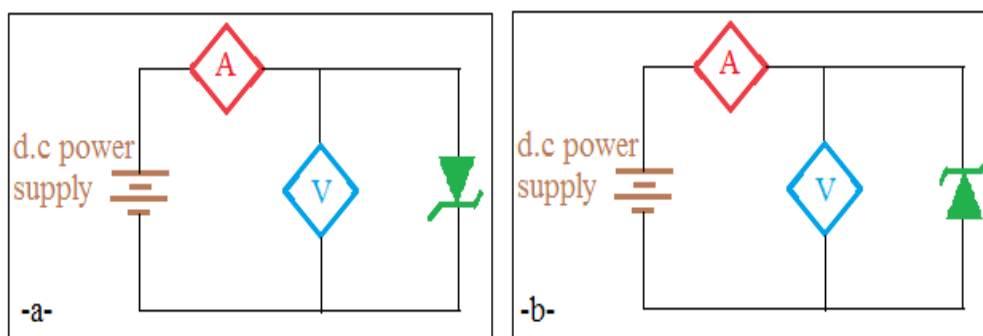


**Fig. 2.** Circuit diagram of  $I - V$  measurement under a-forward b-reverse-bias.

$I - V$  measurements can be determined under lighting for the Al/a-Se/Au junction, prepared with different thicknesses and AT. When they were exposed to Halogen lamp type Philips (120W) with different intensities (160, 230, and 400)  $\text{mW/cm}^2$  using d.c.. power supply, digital Picometer and voltmeter as displayed in figure 3, under bias voltage from (0) to (1) Volt.

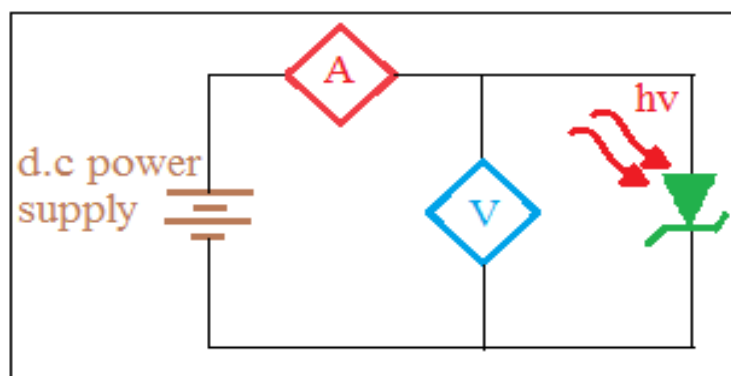


**Fig. 3.** Electric circuit scheme for  $I - V$  measurement of S. junction Solar Cell under illumination.

### 3. Results and discussions

M.S. contact in electronic devices is its D.C. electrical characteristic, and an S. barrier is determined by a function of the current ( $I$ ) at the junction versus the applied Voltage ( $V$ ) (Takshi 2007). When the current is a linear function of the Voltage, the link is named an O.C. While S. contact gets on when the M.S. contact is non-linear (not Ohmic). In this paper, the same terminology is used to differentiate a linear behavior from a non-linear behavior  $I$ - $V$  function, which can be dependent on two terms: S. and O.C.

#### 3.1 OC of Al/a-Se/Al junction

Figure 4 gives the  $I - V$  Characteristic for Al/a-Se/Al junction in forward and reverse bias. A linear  $I$ - $V$  can be seen from this figure. This behavior is interpreted according to (Hossain *et al.*, 2008), such that the Al has a small series resistivity, which makes it operate as an O.C. metal. In this case, the Al/a-Se/Al diode device gave a good *Ohmic junction* due to the lack of voltage barrier between Al and a-Se and the high conductivity of a-Se. This result is in agreement with (Oberafo & Mukolu 1994).

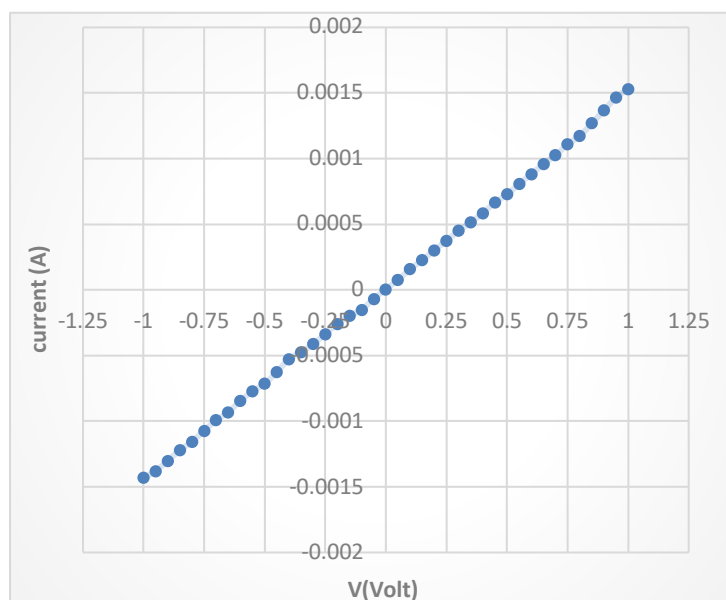


**Fig. 4.** I-V properties of Al/a-Se/Al OC

The analysis of the I-V characteristics is displayed in figure 4 for forward and reverse biasing at R.T. and (300) nm thickness. As shown in the above figure, the O.C. can be observed when I-V characteristics have non-rectifying behavior, which appeared as a linear behavior, as in ref. (Abdul Almohsin *et al.*, 2012).

### 3.2 I – V Characteristics Au/a-Se/Al S. barrier

I – V properties for S.C. can be obtained by using a fixed illumination. Commonly of known intensity. The resistive load varies between open circuit and short circuit settings, also can be measured the Voltage and the current out across the solar cell (Wolf & Rauschenbach, 1963). These measurements which apply to the solar cell are normal P.V. mode of operation and I – V properties called by photovoltaic output characteristic (Mahesha *et al.*, 2008).

In the beginning, experimental attempts were carried out for S. diode preparation by evaporating a gold to construct a 50nm of thickness layer under different thicknesses (300, 500, and 700nm) Se films, then an Al layer, as an O.C., with 300nm of a thickness (Fdhala, M.M, 2012).

Preparation with such a specification lead to distorted layers of the resulted device. It is believed that the collision between Se atoms (high energy) and Au atoms caused an extrusion then the film layers were destroyed, as shown in figure 5.

Another attempt was conducted using Cu, then W, separately as two substrates (plats), representing a pole for S. diode. Results for this method are given in Figures 6 and 7 for W and Cu, respectively. These two figures show only Ohmic properties for current. This was because the selected thicknesses for Sckottky metal are more significant than that for the Se that should give an O.C.

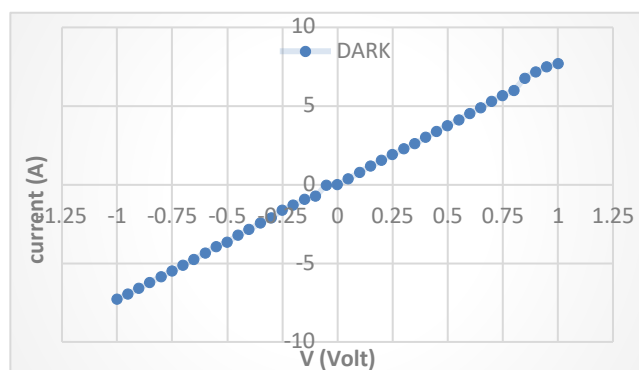


**Fig. 5.** The I-V properties of Au/a-Se/Al for forward and reverse biasing at room T and (300) nm thickness.

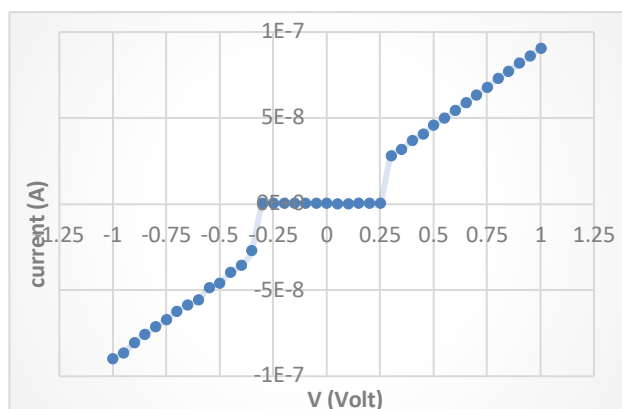


**Fig. 6.** The I-V Characteristic of W/a-Se/Al for forwarding and revers are biasing at room T and (300) nm thickness.

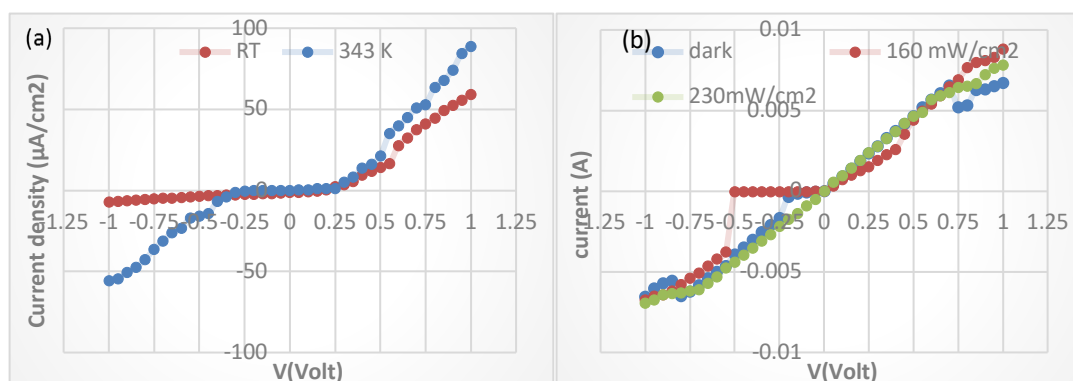


**Fig. 7.** The I-V properties of Cu/a-Se/Al for forward and reverse biasing, at R.T. and (300) nm, in;  
 (a) darkness (with and without) annealing, and (b) darkness at different power lighting densities.

Figures (5, 6, and 7) shows different experiments to achieve S. diode, in which clearly that at R.T. with (300) nm of Se layer, in darkness and different power density for illumination results showed the following:

Figure 5; in trying to construct S. barrier, gold metal is used in a down layer for the S. diode, then into it, Se layer, and then aluminum (Al) layer (a sandwich of Ag-Al and Se in between). Results show a linear I-V characteristic behavior. Rearrangement for these layers

by putting Au in up layer for S. diode (the layer which gets on illumination), we observed that this arrangement is suitable to get S. barrier S.C.

Figure 6; Tungsten metal (W) with Se- Al is used and found hard variation in these materials AT. Tungsten has high AT while Se has low AT. That's causes so hard possibility to get S. barrier between them. So overlapping between these layers is not reachable.

Figure 7; Copper metal (Cu) is used, in which results are not acceptable, wherein darkness and illumination O.C. results.

According to the above results, it is found that the suitable use is with Au with up layers for the junction and the succeeds arrangement is (Al/a-Se/Au), which is used to prepare and then study the S. barrier S.C. in the following section.

### 3.3 $I - V$ Characteristics of Al/a-Se/ Au S. barrier S.C. under darkness

The important parameters of an S. barrier measured I-V properties which clarifies the behavior of the resulting current with the applied forward and reverse bias voltage. Figure 8 shows I-V properties Al/a-Se/Au S. barrier at forward and change bias voltage for different thicknesses ((a) 300nm, (b) 500nm and (c) 700nm) and A.T.s. In low Voltage, the current change exponentially with Voltage at specific conduction by thermionic emission, which agrees with ref. (Mahesha *et al.* 2008).

Results for the effect of forwarding darkness current are given in figure 8. Which results show that the flow of majority carriers and the applied Voltage injects majority carriers, leading to the decrease of the built-in potential and the depletion layer width. Such that

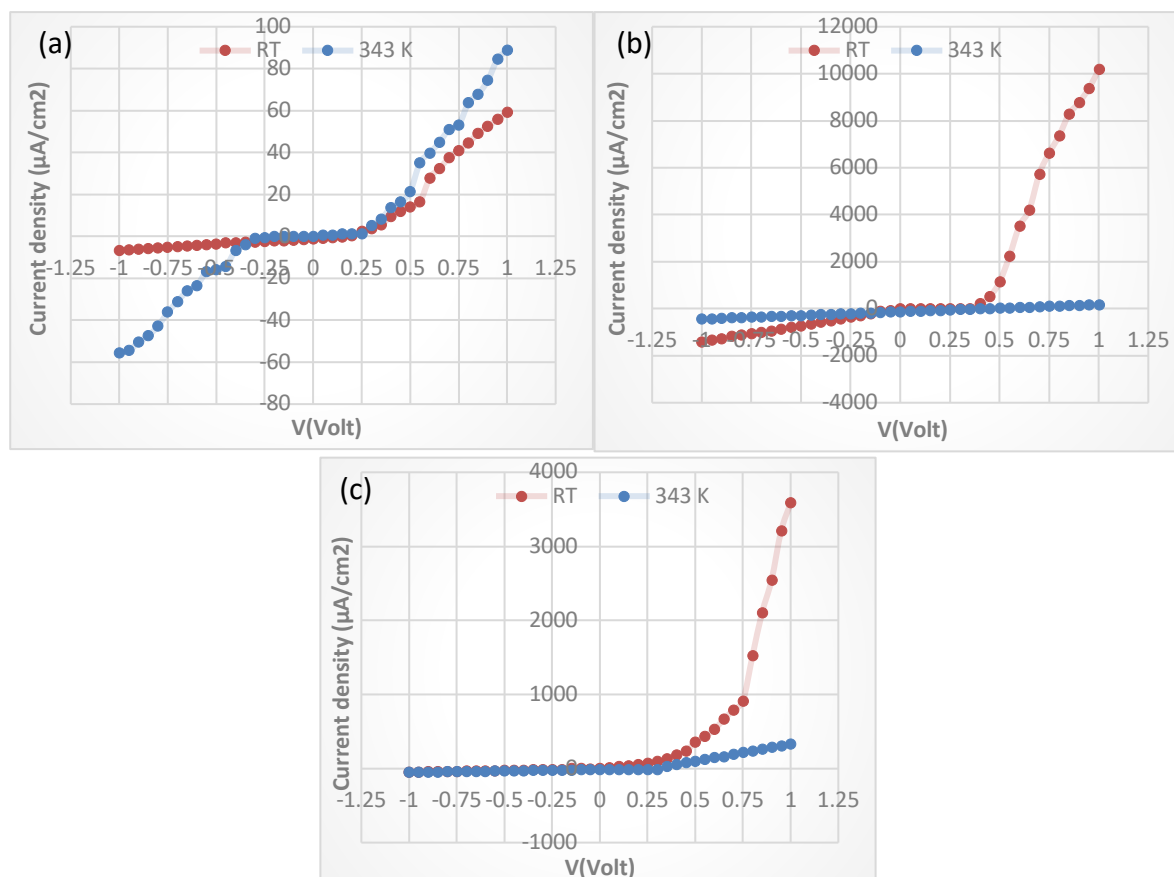


**Fig. 8.**  $I - V$  properties in the darkness for Al/a-Se/Au S. barrier solar cell at forward and reverse bias voltage with thicknesses (a) 300nm, (b) 500nm (c) 700nm, and altered A.T.s.

the current increases with the increase of AT because the increasing of T causes a rearrangement of the interface atoms and reduces the hanging bond, which agrees with ref. (Al-Lamy *et al.*, 2017).

Table 1 shows results for I – V properties for Al/a-Se/ Au S. barrier. The ideality factor (n) values for Al/a-Se/ Au S. barrier are more significant than unity, and close to unity compensate for their non-ideal behavior.

**Table 1.** I – V properties for Al/a-Se/ Au S. barrier S.C. under darkness for a-Se films at different thicknesses and A.T.s.

Thickness (nm)	T <sub>a</sub>	$\phi_B$	n	J <sub>s</sub> ( $\mu\text{A}/\text{cm}^2$ )
300	RT	0.240	2.386	134.17
	343K	0.265	1.860	51.739
500	RT	0.255	2.271	75.694
	343K	0.260	1.548	62.542
700	RT	0.295	2.192	16.088
	343K	0.299	1.395	13.445

The deviation from ideality could be related to more than one reason, such as; the highly disordered nature of the amorphous film, which results in defect states, or the current transport mechanisms such as generation recombination in the depletion region and tunneling out of the barrier, which agrees with ref. (Chaudire *et al.*, 2007). Another cause is that the interfacial oxide layer may cause a higher ideality factor, which concurs with ref. (Hess, 1988). The tunneling through the barrier is possible only in highly doped materials at lower T<sub>s</sub>. Thus, the tunneling mechanism is thought to be out of possibility.

From the above table, the annealing T affects the ideality factor at different thicknesses; the ideality factor behavior is very normal, decreasing with increasing the T of annealing. The same table shows that the T of annealing affects the reverse saturation density; therefore, there is a probable optimum T that gives an optimum saturation current and optimum  $\phi_B$  for Al/a-Se/ Au S. barrier because of chemical reaction at the metal / Se interface. This result agrees with ref. (Yilmaz *et al.*, 2007).

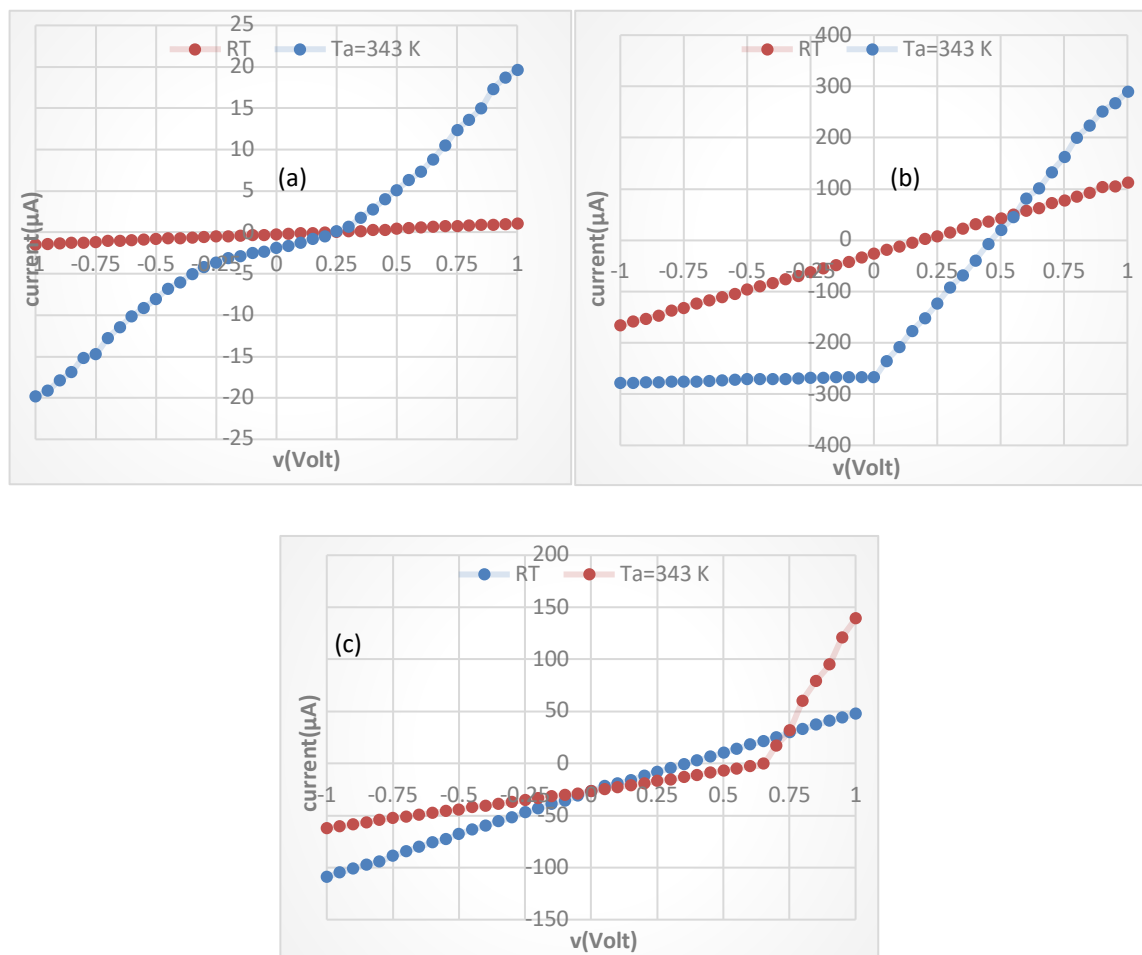
### 3.4 I – V Characteristics for Al/a-Se/Au S. barrier S.C. under illumination

The photocurrent, P<sub>c</sub>, density (J<sub>ph</sub>) with bias voltage (V) of the Al/a-Se/ Au S. barrier at different thicknesses and A.T.s are presented in figures 9,10, and 11. The measurements have been carried out under different power densities equal to (160,230 and 400) mW/cm<sup>2</sup>.

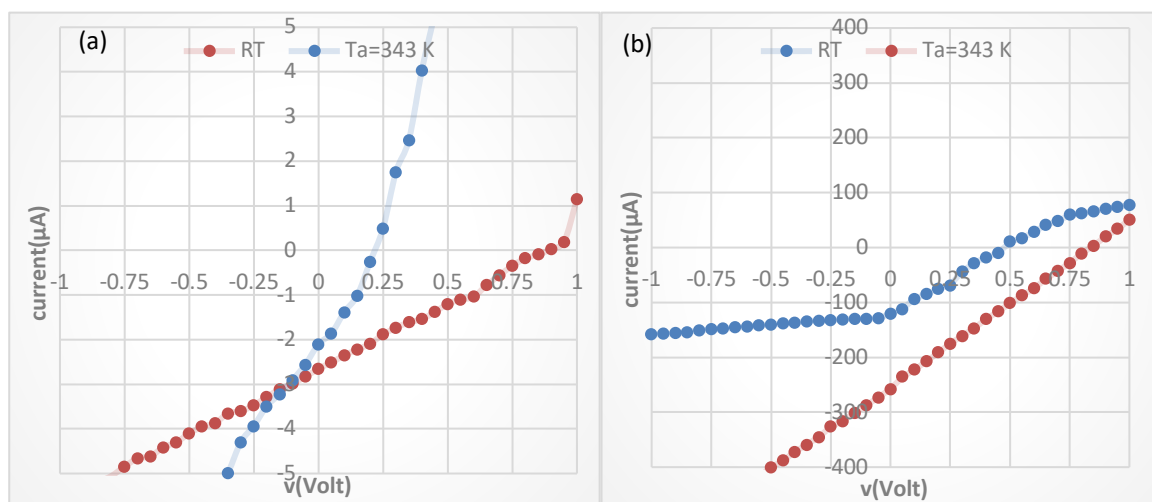
These figures show that the P<sub>c</sub> density increases with increasing the bias voltage, i.e., J<sub>ph</sub> increases with increasing the depletion region width (W).

The depletion region width increases with the increasing the applied reverse bias voltage, which leads to separating the e-h pairs and then increasing the P<sub>c</sub> density. The forward and reverse bias P<sub>c</sub> is a function of the generation and diffusion carriers. So that the P<sub>c</sub> increases with increasing T of annealing and this is accredited to the increase in the size of grain and reducing the boundaries of grain and improvement of a structure, so that due to the rise of the mobility also can increase the P<sub>c</sub> in addition to the increase of the depletion width that due to the increase of the (e-h) pairs creation. Figures 9, 10 and 11 show that the P<sub>c</sub> increases with increasing film thickness and power densities (160, 230, and 400) mW/cm<sup>2</sup>.





**Fig. 9.** *I* – *V* characteristics under illumination (160mW/cm<sup>2</sup>) for Al/a-Se/ Au S. barrier SC at forward and reverse bias voltage with thicknesses (a) 300nm, (b) 500nm (c) 700nm and different ATs.



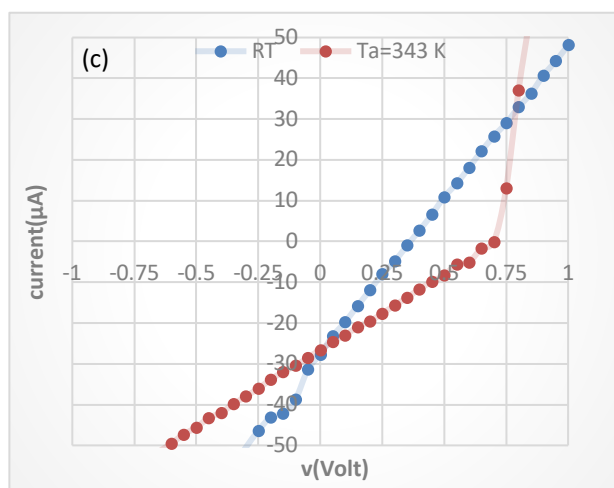


Fig. 10. I – V characteristics under illumination ( $230\text{mW}/\text{cm}^2$ ) for Al/a-Se/ Au S. barrier SC at forward and reverse bias voltage with thicknesses; (a) 300nm, (b) 500nm (c) 700nm and different ATs.

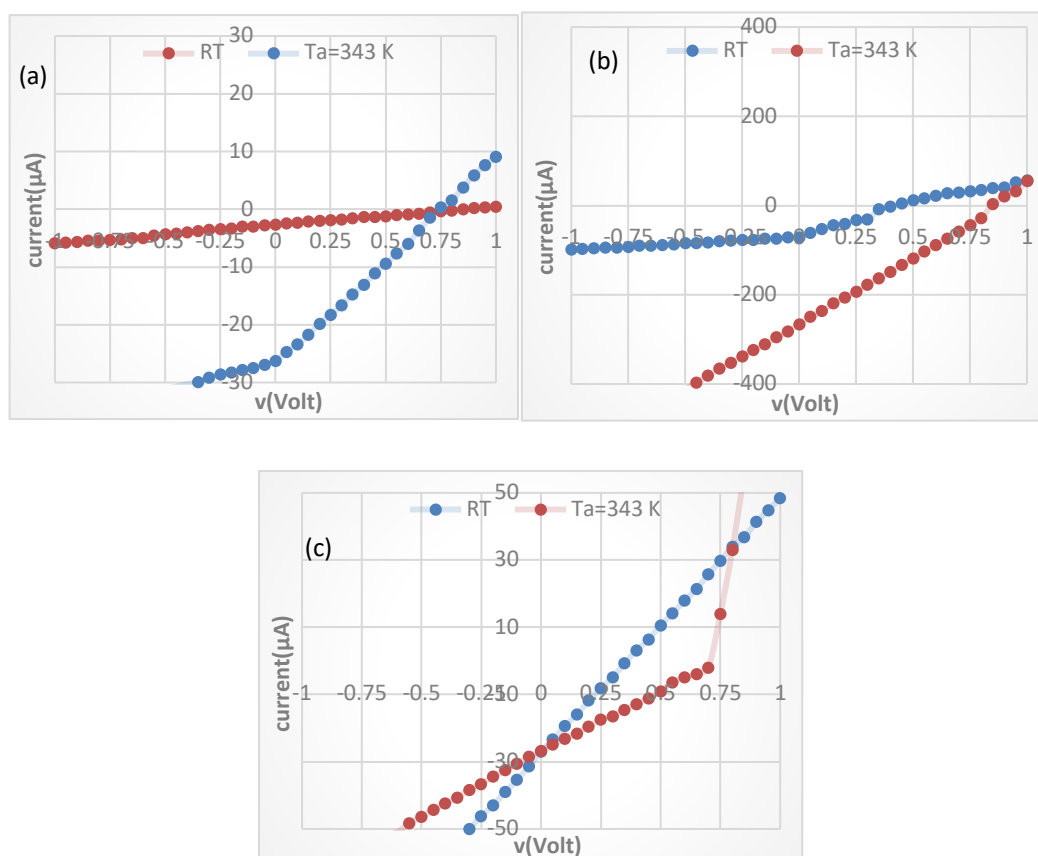


Fig. 11. I – V properties under lighting ( $400\text{mW}/\text{cm}^2$ ) for Al/a-Se/ Au S. barrier SC at forward and reverse bias voltage with thicknesses (a) 300nm, (b) 500nm (c) 700nm and different ATs.

The relationship between current forward bias and Voltage increases exponentially, while in current reverse increased slowly with Voltage and did not show any trend of saturation or sharp break down. So we can see the open-circuit Voltage ( $V_{oc}$ ) rises, which can be related to decreasing the recombination center in terms important the crystal structure similar variation, which agrees with ref. (Al-Lamy *et al.*, 2017).

### 3.5 Short circuit current, open-circuit Voltage, and efficiency measurement for Al/a-Se/ Au S. barrier S.C.

The short-circuit current ( $I_{sc}$ ) and the open-circuit Voltage ( $V_{oc}$ ) are very important parameters because they can determine the region on which the S. barrier operates. It can separate the generated pairs without applying any external field. The ( $I_{sc}$ ) and ( $V_{oc}$ ) curve can be divided into two sections; a saturation section at high illumination intensities and a linear section at low light intensities, as a result of excitation and separation of electrons from their atoms by incident photons which leads to creating e-h pairs and then increases of ( $V_{oc}$ ) and ( $I_{sc}$ ) (Chaudire *et al.*, 2007).

Results given in table 2 show that  $V_{oc}$  is increasing directly with: thickness, AT, and power density (160, 230, and 400) $mw/cm^2$  for Al/a-Se/ Au S. barrier S.C. This proportionality is attributed to the defects acting as capture centers to generate carriers, increasing recombining and then-current value. From increasing ( $I_{sc}$ ) and ( $V_{oc}$ ) with increasing the thickness and AT, the efficiency  $\eta$  increased directly with both thickness and AT of Al/a-Se/ Au S. barrier S.C.

**Table 2.** VOC,  $I_{sc}$ ,  $V_{max}$ ,  $I_{max}$ , F.F., and efficiency ( $\eta\%$ )for Al/a-Se/ Au S. barrier S.C. with different thicknesses, A.T.s, and power densities.

Lighting power density		160 mW/cm <sup>2</sup>						
Thickness(nm)	T <sub>a</sub> (K)	V <sub>oc</sub> (mV)	I <sub>sc</sub> (mA)	F.F	V <sub>m</sub> (mV)	I <sub>m</sub> (mA)	$\eta\%$	
300	RT	190	0.00025	0.211	100	0.0001	0.0318	
	343	240	0.0019	0.329	150	0.0010	0.4778	
500	RT	180	0.0260	0.269	90	0.0140	4.0130	
	343	480	0.0120	0.316	260	0.0070	5.7960	
700	RT	380	0.0280	0.125	220	0.0060	4.0640	
	343	700	0.0270	0.118	400	0.0056	7.1340	
Lighting power density		230 mW/cm <sup>2</sup>						
Thickness(nm)	T <sub>a</sub> (K)	V <sub>oc</sub> (mV)	I <sub>sc</sub> (mA)	F.F	V <sub>m</sub> (mV)	I <sub>m</sub> (mA)	$\eta\%$	
300	RT	240	0.0021	0.327	150	0.0011	0.365	
	343K	850	0.0026	0.285	450	0.0014	1.396	
500	RT	400	0.0070	0.54	300	0.0050	3.344	
	343K	850	0.0250	0.264	400	0.0140	12.407	
700	RT	360	0.0280	0.248	200	0.0125	5.539	
	343K	700	0.0271	0.267	360	0.0140	11.166	
Lighting power density		400 mw/cm <sup>2</sup>						
Thickness(nm)	T <sub>a</sub> (K)	v <sub>oc</sub> (mV)	I <sub>sc</sub> (mA)	F.F	V <sub>m</sub> (mv)	I <sub>m</sub> (mA)	$\eta\%$	
300	RT	900	0.0026	0.278	500	0.0013	0.828	
	343K	760	0.0260	0.283	400	0.0140	7.134	
500	RT	400	0.0270	0.28	300	0.0101	3.86	
	343K	850	0.2600	0.027	400	0.0150	7.643	
700	RT	360	0.0272	0.367	200	0.0180	4.585	
	343K	710	0.0474	0.39	300	0.0400	15.286	

The last table gives the short circuit current as a function of solar irradiance for cells used in measurements presented in figures 9, 10, and 11. These values show that at low series resistance, cells exhibit a linear relationship between short circuit current and solar irradiance up to (160, 230 400 mW cm<sup>-2</sup>); this agrees with ref. (Wolf *et al.*, 1963).

#### 4. Conclusions

The value of the building-in potential for Al/Se/Au S. barrier increases with the increasing thickness and A.T.s, also the S. barrier height increases the thickness and AT.

*I – V* Characteristic Al/a-Se/ Au S. barrier at forward and reverse bias voltage, in low Voltage, the current change exponentially with Voltage signifying the conduction by thermionic emission. The values of the ideality factor(n) for Al/a-Se/ Au S. barrier is found to be larger than unity, and it is close to unity when increased the thickness and A.T.s. Short circuit current density ( $J_{sc}$ ), open-circuit Voltage ( $V_{oc}$ ), and efficiency ( $\eta\%$ ) increase with the increasing thickness and AT.

#### ACKNOWLEDGEMENTS

The authors would like to thank Mustansiriyah University ([www.uomustansiriyah.edu.iq](http://www.uomustansiriyah.edu.iq)) and the University of Baghdad, Baghdad – Iraq, for their support in the present work.

#### References

- Abdul Almohsin, S., AL-Mutoki, S.M. & Li, Z. (2012)** Al/PANI-MWNT/Au-plastic S. diode solar cells. *Journal of the Arkansas Academy of Science*; 66: 36-40.
- AbuShama, J., Johnston S, Ahrenkiel R, & Noufi R. (2002)** National renewable energy laboratory: Deep level transient spectroscopy and capacitance-voltage measurements of Cu (In, Ga) Se<sub>2</sub>. *IEEE; P.V. Specialists: Conference, New Orleans, Louisiana*.
- Al-Lamy, H.K., Al-Ansari, R., Awadh, J.H. (2017)** D.c.. conductivity, Hall effect of amorphous arsenic and I-V characteristic of a- As/c-Si heterojunction. *Journal of Scientific and Engineering Research*, 4(8):50-53.
- Chaudire, M., Vohra, A. & Chakarvarti, S.K. (2007)** Effect of diameter on I–V characteristics of template synthesized Cu–Se nano/microstructures. *Journal of Materials Science: Materials in electronics*, 17(12):993-997.
- Mutar, F.M. & Hemed A.A., (2014)** Effect of thermal annealing on a-Se thin films' structural, optical, and electrical properties. *Advances in Physics Theories and applications*; (31): 16-24.
- Fdhala, M.M., (2011)** Electronic transport in Al/a-Se /M S. diodes. A thesis submitted to the college of Science for women; University of Baghdad, Baghdad, Iraq.

**Hamza, M.f. (2010)** Electronical, optical and structural properties of ZnSe thin films. A thesis submitted to the committee of the College of Science; University of Baghdad, Iraq.

**Hemed, A.A., Fdhala, M.M. & Khorsheed, S.M. (2022)** Modified superstructure fiber Bragg grating for a filter application; Kuwait J. of Science; (49)1: 1-18.

**Hemed, A.A, Ghayib Z.R. & Rashid, H.G. (2021)** Controlling a chaotic anti-synchronized oscillator by a phase interplayed optical injected seed with an FBG sensor. Journal of Physics: Conference Series; 2nd International Conference on Physics and Applied Sciences (ICPAS 2021), College of Education, Mustansiriyah University, Baghdad, Iraq (1963): 012063.

**Hemed, A. A & Abbas, R.S. (2020)** Enhanced emission perturbations associated with mixed optical injection in the laser diode. AIP Conference Proceedings; (2290)1: 050021.

**Hess, K., (1988)** Advanced theory of semiconductor devices. Wiley-IEEE, ISBN: 978-0-780-33479-3, Appendix G.

**Hossain, M.S., Islam, R. & Khan, K.A. (2008)** A.c. conductivity and dielectric behavior of chalcogenide Gex Fex Se100-2x thin films. Chalcogenide letters; 5(1): 1 – 9.

**Khan, M.R.H, Detchprohm, T., Hacke, P., Hiramatsu, K. & Sawaki N. (1995)** The barrier height and interface effect of Au-n-GaN S. diode. Journal of Physics D: Applied Physics; (28) 1169.

**Mahesha, M.G., Kasturi, V.B. & Shtvakumar, G.K. (2008)** Characterization of thin-film Al/p-CdTe S. diode. Turkish J. Phys.; (32) 151 – 156.

**McEvoy, A., Markvart, T. & Castaner, L. (2011)** Practical handbook of P.V.s, 2nd Edition: Fundamentals and Applications. Elsevier, Academic Press.

**Nelson, J. (2003)** The physics of solar cells. The Imperial college Press. London. Pp. 200.

**Oberafo, A.A. & Mukolu, A.I. (1994)** The nature of some contacts (Al, In, Ge, Sb, and Bi) to selenium films; Turkish J. of Physics; (18) 727-733.

**Parlakturk, F., Agasiev, A., Tataroglu, A., & Altindal, S. (2007)** Current-voltage (I-V) and capacitance-voltage (C-V) characteristics of Au/Bi<sub>4</sub>Ti<sub>3</sub>O<sub>12</sub>/SnO<sub>2</sub> structures. Chemistry, Gazi University Journal of Science; 20(4): 97-102.

**Wolf, M. & Rauschenach, H. (1963)** Series resistance effects of solar cell measurements. Advanced energy conversation, (3) 455-479.

**Sumaryada, T., Sofyan, A. & Syafutra, H. (2019)** Simulation of the extra-terrestrial and terrestrial performance of GaAs/Ge dual-junction solar cells. Kuwait J. Sci. 46 (4) pp. 58-65.

**Sze, S.M. (1981)** Physics of semiconductor devices: 2nd Edition. New York. Pp.150.

**Takshi, A. (2007)** Organic metal-semiconductor field-effect transistor (MOSFET). Ph.D. thesis; University of British Columbia. Canada.

**Yilmaz, K., Parlak, M. & Ercelebi, C. (2004)** Investigation of P.V. properties of amorphous InSe thin-film based S. device. Semiconductor Science and Technology; 22(12).

**Zeghbrock, B.V. (2004)** Principles of semiconductor devices. Colorado, USA. Pp.15.

**Submitted:** 26/02/2021

**Revised:** 12/05/2021

**Accepted:** 21/05/2021

**DOI:** 10.48129/kjs.12729